Journal of Engineering Physics and Thermophysics, Vol. 77, No. 6, 2004

INVESTIGATION OF THE PROPERTIES OF A MAGNETOFLUIDIZED BED AND DEVELOPMENT OF A NEW GAS PURIFICATION TECHNOLOGY BASED ON THEM FOR SIMULTANEOUS REMOVAL OF SOLID AND GASEOUS SUBSTANCES FROM HOT WASTE GASES

A. F. Dolidovich

UDC 66.096.5:66.074.5.081.3.097

The results of investigation of the influence of the mechanical, thermal, structural, catalytic, and regenerative characteristics of granular oxide catalysts on the efficiency of decontamination of volatile organic substances in the catalyst unit and of the filtration rate, amount, and concentration of dust, the size of filter particles, the direction and intensity of a magnetic field, and other parameters on the behavior of the particles, the structure, the porosity, the resistance, the optimum fluidization rates, and the efficiency of collection of dust in magnetofluidization of magnetic particles have been given. The diagram and operating principles of a new technology for simultaneous decontamination of volatile organic matter and collection of dust have been presented.

Hot waste gases of many industrial processes with a temperature to 900°C are contaminated with volatile organic substances and dust, whose concentrations vary over a wide range from zero to tens of g/m^3. Theory and industrial practice offer a few methods of removal of such pollutants from hot gases, including thermal and catalytic decontamination of gaseous organic matter and inertial electrostatic dust control as well as filtration of the gases through ceramic, fiber, or granular filters for collection and removal of finely divided dust. Each of the methods mentioned above possesses its inherent advantages and disadvantages, a detailed discussion of which is beyond the scope of the present paper, where the emphasis is on the development of new methods and equipment that are based on the principles of filtration of hot gases through a granular bed.

It is well known [1–3] that the method of filtration of gases through fixed and fluidized beds is widely used to monitor the emission of dust and has demonstrated its sufficient efficiency for particles with a wide range of sizes. Filtration through a fixed bed ensures a sufficient efficiency of dust collection for relatively high flow rates of the gas. It is particularly suitable for operation under the conditions of higher-than-average temperatures and pressures. However, filtration through a fixed granular bed is characterized by an unstable state, since such a filter is gradually and to an increasingly greater extent clogged with the collected dust and the resistance of the bed continuously grows. In this connection, the granular bed must be regenerated or be replaced by a new one. The inevitable consumption of time by this procedure makes the operating costs of the process of gas purification higher. Furthermore, filters with a fixed bed are unsuitable for operation with sticking-together volatile ashes and similar substances.

One possible means of overcoming this drawback is the operation of a granular filter in the regime of a fluidized bed, which allows continuous removal and introduction of a filter medium. Fluidized-bed filters possess the advantages of continuous operation with higher flow rates of the gas; they are more suitable in situations in which the adhesion of dust to the surface of a filter medium presents operational problems. However, fluidized-bed filters have a serious disadvantage and are less efficient in the regime of bubble nucleation in which the rate of flow of the gas through the bubbles is fairly high, which adversely affects the contact between the dust in the gas flow and the fluidized particles serving as dust collectors.

In general, an ideal and highly efficient device for granulation filtration could be a filter with a fluidized bed operating without gas bubbles. The characteristics of homogeneous gas filtration can be ensured by application of ex-

---

A. V. Luikov Heat and Mass Transfer Institute, National Academy of Sciences of Belarus, 15 P. Brovka Str., Minsk, 220072, Belarus; email: adol@hmti.ac.by. Translated from Inzhenerno-Fizicheskii Zhurnal, Vol. 77, No. 6, pp. 59–73, November–December, 2004. Original article submitted November 11, 2003.

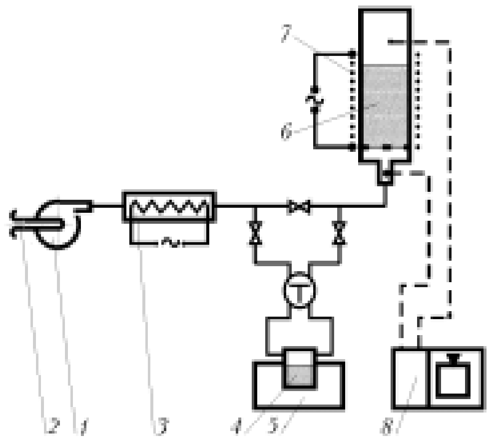

Fig. 1. Experimental setup for investigation of catalytic oxidation of volatile organic substances.

ternal magnetic forces to a bed of particles possessing magnetic properties [4–11]. A number of researchers [5, 6, 12, 13] checked the possibility of using the principle of magnetically stabilized filters for collection of dust and confirmed its high potential for these purposes. However, most of the investigations were limited to a narrow range of velocities of the gas and a low intensity of the external magnetic fields applied.

The present paper seeks to investigate the filtration of dust in a filter with a magnetically stabilized fluidized bed in an extended range of operational variables, to check their influence on the efficiency of dust collection in greater detail, and to develop, on this basis, a new technology for removal of gaseous and solid substances from "hot" waste gases.

Experimental. In investigations on catalytic oxidation of organic matter, we used the experimental setup presented in Fig. 1 and described in [14]. Different types of granular aluminum gamma-oxide catalysts with the average particle-size distribution lying in the ranges $0.4 \le d_s \le 0.6$ mm, $0.6 \le d_s \le 1.0$ mm, $1.0 \le d_s \le 1.6$ mm, $1.6 \le d_s \le 2.0$ mm, $2.0 \le d_s \le 2.5$ mm, and $2.5 \le d_s \le 3.0$ mm were used as the materials tested for mechanical, structural, catalytic, regenerative, and other properties. Representatives of aldehydes, ketones, esters and ethers, alcohols, aromatic hydrocarbons, and their multicomponent mixtures characteristic of the waste gases of different industries in composition were used as volatile organic substances. The experimental procedure was as follows. Air was fed to the setup by fan 1 equipped with flowmeter 2, was heated by the electric heater 3, was saturated with the vapor of the organic substances in saturator 4 located in thermostat 5, and arrived at column 6 with a fixed or fluidized catalyst bed. The reactor consisted of a quartz-glass column with a perforated grid (free cross-sectional area 1.5%) and was equipped with the external electric heater 7 intended for controlling the temperature of catalytic oxidation of organic substances. The temperature of the catalyst bed was measured by thermocouples at different heights of the bed. The gases were analyzed at entry into the catalyst bed and at exit from it by chromatograph 8.

An experimental device used to investigate the efficiency of filters with a magnetofluidized bed and partially similar to the setup described in [8] is presented in Fig. 2. The device consists of several independent units, such as the air feeding system, the quartz-glass column with a fluidized bed, the heater, the dust generator, the system of purification of gases escaping from the column, the Helmholtz electromagnet, the system for measurement of the resistance and temperature of the bed, and the system of analysis of the particle size and density.

The column for fluidization consisted of a transparent quartz-glass tube with an inside diameter of 101.6 mm. The pressure difference in it was measured by two transducers located at distances of 6 and 127 mm from the gas-distributing grid. In each experiment, the quantity ΔP was recorded with increase and decrease in the velocity U. The ΔP values measured for an increasing velocity U were used for determination of $U_{\min,f}$, and those measured for a decreasing velocity U were used for determination of $U_{\min,b}$ from the point of intersection of the experimental curve $\Delta P = f(U)$ and the values of W/A. The porosities ε of the bed were determined from the measurements of the bed's height and from the data of measurements of ΔP that corresponded to the portion of the bed located between heights of the bed of 31.75 and 101.6 mm above the gas-distributing grid.

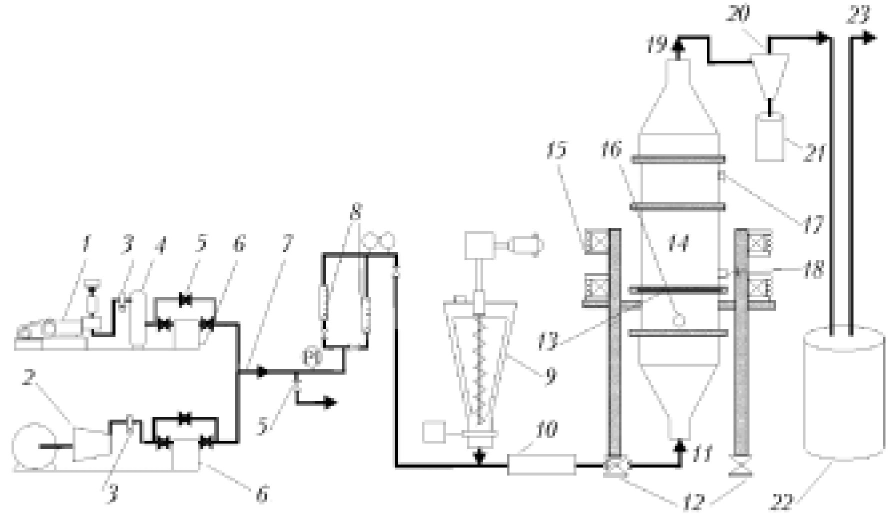

Fig. 2. Experimental setup for investigation of the operating efficiency of a filter with a magnetofluidized bed: 1) piston compressor; 2) rotary compressor; 3) separators; 4) air receiver; 5) by-pass valves; 6) drainage; 7) general outlet of air; 8) rotameter; 9) dust generator; 10) heater; 11) injection of the gas; 12) adjustable posts; 13) gas-distributing grid; 14) column; 15) electromagnet; 16) temperature sensors; 17) injection of particles; 18) ejection of particles; 19) outlet of the gas; 20) cyclone separator; 21) tank for collected particles of the bed; 22) tank for collection of dust; 23) air to be ejected.

The section of the column with the test bed passed through the central gap of the electromagnet of diameter 355.6 mm. The calculations showed that the magnetic field inside the particle bed was homogeneous with a deflection of 1%. In most of the experiments, the magnetic lines of the Helmholtz coil coincided with the direction of the air flow. Some experiments where the direction of the magnetic lines was opposite to the direction of the air flow showed no significant differences in the values of the measured parameters, which were much higher than the accuracy of experiment.

Ferromagnetic particles of iron spheres with an average diameter of d_s = 733 and 1511 μm were used as the filter bed and material. In most of the experiments, the bed's height was 85 and 100 mm. Monofractions of aluminum oxide and talc were used as finely divided dust particles whose size was d_d = 20 and 2.0 μm respectively. The concentration of the dust in the incoming flow C_{in} of the gas varied over a wide range (0–7.15 g/m^3) at a prescribed air temperature.

Before each experiment, we charged flushed and screened iron spheres of required volume into the column. The flow rate of the gas and its temperature were controlled by the compressor and the heater. The dust generator fed dust particles with a prescribed concentration to the granular filter with an energized or de-energized electromagnet. In the course of the filtration experiments, filter particles could be in the state of a fixed, fluidized, or magnetofluidized bed. We sampled the dust simultaneously at entry into the filter and at exit from it. Also, we measured the temperature, the height of the bed and its resistance, and the particle velocity as a function of the force of the magnetic field applied. Each experiment lasted for several hours.

Experimental variables were the velocity of the gas, the height of the filter-particle bed (expressed in the form of the equivalent height of a fixed bed), the size of the ferromagnetic particles (filter medium) and the dust, and the intensity of the magnetic field. In all, we performed 520 experiments, in which the range of variation of the variables was $0 \le U \le 4.0$ m/sec, $85 \le h \le 100$ mm, and $0 \le H \le 20{,}000$ A/m.

Results and Discussion. *Efficiency of Decontamination of Volatile Organic Compounds in a Fixed and Fluidized Catalyst Bed.* To find the basic structural and operating parameters of a catalytic filter for decontamination of organic substances and to investigate its efficiency we performed a series of experiments with the use of catalysts developed at the G. K. Boreskov Institute of Catalysis of the Siberian Branch of the Russian Academy of Sciences; some results of these experiments are given below.

TABLE 1. Characteristics of Granular Catalysts Used for Decontamination of Volatile Organic Substances

Characteristics	$CuCr_2O_4$	$MgCr_2O_4$	$Cu_xMg_{1-x}Cr_2O_4$	Fe_2O_3
Carrier	γ-Al_2O_3	γ-Al_2O_3	γ-Al_2O_3	γ-Al_2O_3
Granule diameter, mm	1.0–1.6	1.0–1.6	1.0–1.6	1.0–1.6
Volume weight, kg/m^3	1040	1070	1100	880
Specific surface, m^2/g	107	119	131	208
Mass of the active component, wt. %	20.7	25.0	22.4	3.0
Mechanical strength crush strength, MPa:				
average	–	45.2	48.9	31.2
minimum	21.0	25.9	23.1	19.2
shock strength, J/m^2	9.4	9.24	9.3	–
Relative volume of pores, %, with a radius of, Å:				
30—60	7	6	13	85
60—110	81	62	79	10
100—180	7	17	6	2
Activity of the catalyst in oxidation of butane, 10^{-2} cm^3 /(g·sec)				
at 573 K	0.30	0.32	0.34	–
at 673 K	2.50	2.82	2.34	0.93
Temperature of attainment of a 50% conversion of CO, K	527	613	511	515

TABLE 2. Temperatures and Efficiencies of Deep Catalytic Oxidation of Certain Organic Compounds

Volatile organic substances	$CuCr_2O_4$ $d_s = 2.0–2.5$ mm		$MgCr_2O_4$ $d_s = 1.0–1.6$ mm		$MgCr_2O_4$ $d_s = 2.0–2.5$ mm		$Cu_xMg_{1-x}Cr_2O_4$ $d_s = 2.0–3.0$ mm	
	T, K	η, %	T, K	η, %	T, K	η, %	T, K	η, %
Acetone	600	99.8	623	100	650	99.9	640	100
Ethyl acetate	623	99.8	600	99.9	640	100	630	100
Toluene	630	99.7	650	99.6	673	99.5	645	99.1
Butyl acetate	620	99.9	590	99.6	635	99.8	625	100
Benzene	623	99.8	623	99.7	630	99.9	623	100
Turpentine	630	99.6	630	99.5	630	99.7	630	99.9
White spirit	600	100	600	99.9	623	100	600	100

Structural, Physicochemical, and Mechanical Properties of the Catalysts. The results of investigations of certain characteristics of these heterogeneous catalysts are generalized in Table 1. The data given in it show that the catalysts have a fairly developed specific surface area (from 107 m^2/g for $CuCr_2O_4$ to 208 m^2/g for Fe_2O_3), a high catalytic activity in oxidation of butane (from $0.93 \cdot 10^{-2}$ cm^3/(g·sec) for Fe_2O_3 to $2.82 \cdot 10^{-2}$ cm^3/(g·sec) for $MgCr_2O_4$) and in conversion of carbon monoxide (with temperatures of attainment of a 50% conversion from 511 K for $Cu_xMg_{1-x}Cr_2O_4$ to 613 K for $MgCr_2O_4$), and a high mechanical strength (the average mechanical crush strength varies from 31.2 MPa for Fe_2O_3 to 48.9 for $Cu_xMg_{1-x}Cr_2O_4$, whereas the average shock strength varies from 9.24 J/m^2 for $MgCr_2O_4$ to 9.47 J/m^2 for Cr_2O_4). The experiments on lifetimes, performed under rigid conditions of a high-temperature fluidized bed in a pilot reactor, have demonstrated that these catalysts preserve their catalytic activity for a long period (longer than 3.5 thousand h).

Catalytic Characteristics of the Catalysts and Efficiency of Purification of Gases of Volatile Organic Substances. We investigated the efficiency of catalytic oxidation of the compounds mentioned above and of other individual organic compounds and their mixtures in passage through a heated fixed or fluidized catalyst bed; some results of these investigations are presented in Table 2 and Fig. 3. From the data presented it is clear that the efficiency of catalytic decontamination of volatile organic matter in the fluidized bed is somewhat lower than that in the fixed bed be-

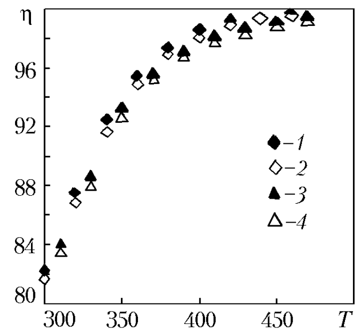

Fig. 3. Efficiency of decontamination of organic volatile substances vs. temperature of a fixed fluidized catalyst bed: 1) $CuCr_2O_4$ and $U < U_{min,f}$; 2) $CuCr_2O_4$ and $U = U_{min,f}$; 3) $MgCr_2O_4$ and $U < U_{min,f}$; 4) $MgCr_2O_4$ and $U = U_{min,f}$ [1, 3) fixed bed; 2, 4) fluidized catalyst bed]. h = 100 mm; η, %; T, ^oC.

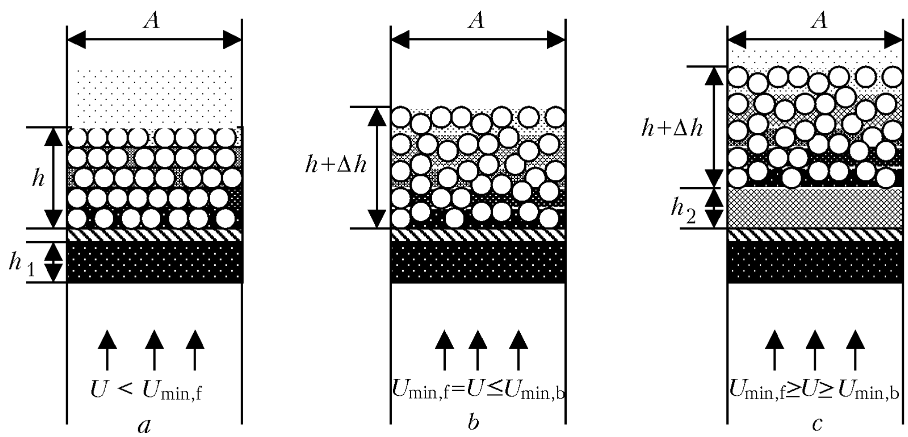

Fig. 4. Collection of dust in fixed (a), fluidized (b), and magnetofluidized (c) beds.

cause of the lower porosity and better contact of the gases containing organic matter and the particles of the bed in the latter. These results also show that, in the temperature range 300–500^{o}C, all types of the investigated gaseous organic compounds, including such a representative (oxidized to the smallest extent by the catalysts used) of aromatic hydrocarbons as toluene, are completely oxidized and removed from the waste gases and the efficiency of decontamination of the volatile organic matter in the fluidized and fixed bed approaches 100%.

Efficiency of Collection of Dust in a Magnetofluidized Bed. Certain General Propositions of Filtration of a Dust-Gas Flow through a Granular Bed and of Collection of Dust. In general, of greatest appeal for removal of dust from industrial gases are such filters, including granular ones, that have a large capacity, a low hydrodynamic resistance, the possibility of operating in a wide range of operating velocities and flow rates, and, consequently, a long lifetime and low operating costs. Furthermore, an important characteristic of any filter is the possibility of regenerating a filter medium and the simplicity of this procedure. In this context, it is of interest to consider briefly the operating characteristics of the existing granular filters.

The mechanisms by which dust is retained and accumulated in the volume of a granular bed are well known. They include gravitation, inertial collision, deposition and accumulation on the granular surface and in the interpore space, Brownian diffusion, and electrostatic, magnetic, and other effects.

According to Fig. 4a, the accumulation volume of any granular filter is determined in the first approximation by the geometric dimensions of the filter (cross-sectional area A and height h), the particle size d_s, and the porosity of the bed ε, and by the capacity of the space $V_1 = h_1A$ below the gas-distributing grid. In the course of the analysis, we will consider A, d_s, and V_1 to be identical for all types of granular filters.

In filters with a fixed bed, the rate of filtration of the gas U has a rather limited range. It must be higher than the free-fall velocity of the dust U_t but lower than the rate of fluidization of the bed $U_{min,f}$. The particles are immobile, and the accumulation volume of such a bed ($V_c = V_{bed} - V_s$ = const) is determined only by its porosity, having a constant value. In filtration of a gas-dust flow through such a filter, the dust, under the action of the forces of gravity, collision, and trapping, is first collected in the interpore space of the lower interlayers of the granules, where it is gradually compacted, reducing the cross-sectional area of the pores and increasing the hydrodynamic resistance of the bed. Then, due to the growth in the gas velocity in these pores, the particles gradually diffuse into the following granular interlayers under the action of aerodynamic forces and suffosion. When the dust fills the interpore space of the highest granular interlayer and reaches the upper plane of the bed, its re-removal and accordingly a reduction in the dust-collecting capacity of the filter will begin. Simultaneously with the process of collection of dust in the granular bed and the growth in its resistance and due to the fact that the amount of re-removed dust is smaller than the amount arriving at the filter inlet, accumulation of the dust in the subgrid space begins, which increases the resistance of the filter even more. Thus, irrespective of other influencing factors, filters with a fixed bed have a rather limited accumulation volume as compared to other granular filters and a higher resistance, which substantially limits the possibilities of their industrial application. Knowing the values of V_{bed}, d_s, ρ_s, and V_s, we can find V_c, and from V_c, C_{in}, d_d, and ρ_d we can find the mass of the collected particles m_c and the time τ_p of protective action of the filter up to the re-removal of the dust from its surface. The appearance of the re-removal of dust with a maximum growth in ΔP indicates that the filter is totally clogged and it is necessary to regenerate the filter medium. For this purpose the filter must be put out of operation.

As is well known [2, 5], a fairly high efficiency of collection of dust by a filter with a fluidized granular bed can be maintained in a comparatively narrow range of operating velocities from the rate of minimum fluidization $U_{min,f}$ to the rate of minimum bubble nucleation $U_{min,b}$. When $U_{min,f}$ is attained, the bed expands and becomes fluidized; its height h and, consequently, porosity ε increase as compared to the values in a fixed bed (Fig. 4b). The accumulation volume V_c of the bed also proportionally increases. The expression proposed in [1] for calculation of the porosity and, accordingly, the accumulation volume of the fluidized bed has the form

$$\varepsilon = \left(\frac{18\mathrm{Re} + 0.36\mathrm{Re}^2}{\mathrm{Ar}} \right)^{0.21} . \quad (1)$$

The mechanisms of retention and accumulation of dust in the space of fluidized and fixed beds are analogous. However, in connection with the fact that the particles have become suspended and mobile, their mixing in the fluidized bed begins. As a consequence, particles from the lower regions of the bed, together with the trapped dust, rise to the bed's surface and re-removal of the dust begins. Furthermore, when the rate $U_{min,b}$ is attained, a certain part of the gas is filtered through the bed in the form of bubbles, thus adversely affecting the contact between the gas and the granules and, consequently, reducing the efficiency of collection. Thus, filters with a fluidized bed, despite the large accumulating volume, have a very limited range of operating velocities and a reduced, as compared to a fixed bed, time of protective action to the re-removal of dust. At the same time, these filters are not clogged with dust because of the mobility of the granules; regeneration of the filter medium can be realized directly in the process of collection and the hydraulic resistance of these filters cannot attain such values as those in a fixed filter, which is a substantial advantage over the latter.

Application of the external magnetic field on a bed of ferromagnetic particles (Fig. 4c) introduces another mechanism of collection of dust in a granular filter. The action of magnetic forces makes it possible to monitor many parameters of the fluidized bed that influence the efficiency of collection of dust, including the mobility of granules, the contact of the dust with the granules, the porosity of the bed ε and accordingly the accumulating volume V_c, and the range of operating velocities and flow rates of waste gases. Varying the intensity of the external magnetic field, we can control $U_{min,f}$, $U_{min,b}$, ΔP (to a certain extent), and the state of the bed (fixed, fluidized, magnetofluidized, frozen, etc.). As will be shown below, each of these states can successively be used for collection of dust.

Thus, a granular filter can be considered as a corresponding porous medium and an assembly of individual collectors forming a bed. The efficiency of collection of dust in it can be considered in the form of its accumulation on the surface and in the interpore space between the collectors in passage of a gas-dust flow through them. In many cases, the efficiency of collection under the action of the individual mechanisms mentioned above can easily be determined. To calculate the efficiency of collection of dust under the action of gravitation, Brownian diffusion, and collision, Rajagopalan and Tien [15] proposed the following expressions:

$$(\eta_0)_G = (1-\varepsilon)^{2/3} N_G \,, \tag{2}$$

$$(\eta_0)_D = 4A_s^{1/3} N_{Pe}^{-2/3} \,, \tag{3}$$

$$(\eta_0)_I = 1.5A_s (1-\varepsilon)^{2/3} N_R^2 \,. \tag{4}$$

In designing and calculating filters with a magnetofluidized bed, the most suitable for collection of dust and the best contact between the dust and the bed particles, certain quantities, such as, for example, ΔP, determining the system's hydrodynamic resistance ε, which characterizes the accumulating volume of the bed for different intensities of the magnetic field H and inlet velocity of the gas U, and the rates of minimum fluidization $U_{\text{min,f}}$ and bubble nucleation $U_{\text{min,b}}$ determining the magnetofluidization state must be known a priori. In [12, 13], a number of correlations for calculation of certain parameters of the total collecting efficiency of filters with a magnetofluidized bed

$$\frac{U}{U_{\text{min,f}}} = \frac{\varepsilon_o^3 (1-\varepsilon_{d)}}{(1-\varepsilon_o)\,\varepsilon_d^3} \,, \tag{5}$$

$$\frac{M_0}{\rho_s^{1/2} U_{\text{min,f}}} = \frac{\left\{4\pi\,[1+(1-\varepsilon_o)\,x_0]\right\}^{1/2} (3-2\varepsilon_o)\,\varepsilon_o^2 (1-\varepsilon_d)}{(1-\varepsilon_o)^{3/2}\,\varepsilon_d^3} \,, \tag{6}$$

$$E = 1 - \frac{C_{\text{of}}}{C_{\text{in}}} = 1 - \exp\,[-\lambda h] \,, \tag{7}$$

$$\lambda \cong \frac{\eta}{l_c} = \frac{1}{h} \ln \frac{1}{1-E} \,, \tag{8}$$

$$l_c = d_s \left[\frac{\pi}{6}\,\frac{1}{1-\varepsilon}\right]^{1/3} \,, \tag{9}$$

$$\eta = \lambda l_c = (\eta_0)_{i,I} + (\eta_0)_G + (\eta_0)_D \,, \tag{10}$$

were proposed, where $(\eta_0)_G$, $(\eta_0)_D$, and $(\eta_0)_{i,I}$ can be calculated from expression (2), (3), and (4) or

$$(\eta_0)_{i,I} = (1 + 0.04 N_{\text{Re}_s}) \left[N_{\text{St}} + \left\{ 0.48 \left(4 - 4\frac{N_R}{d_c^*} - \frac{N_R^2}{d_c^{*2}} \right)^{1/2} \right\} \left(\frac{N_R}{d_c^*} \right)^{1.0412} \right] . \tag{11}$$

However Albert et al. did not propose expressions for calculation of the basic quantities, in particular, ΔP, ε, and $U_{\text{min,b}}$, involved in these correlations. Therefore, to appropriately calculate and design a filter with a magnetofluidized bed we must experimentally determine the character of the behavior of particles in the bed and the values of ΔP, ε, $U_{\text{min,f}}$, and $U_{\text{min,b}}$ and find their fundamental dependence on the influencing parameters.

Behavior of the Particles of the Bed in Magnetofluidization. To reveal the influence of the intensity of the magnetic field on the behavior of the bed, including the nucleation and suppression of bubbles in it, the mobility and character of motion of particles at the center and near the walls of the column, the porosity, the minimum rates of fluidization and bubble nucleation, the velocity of rise of the bed above the gas-distributing grid in the form of a solid piston, etc., we carried out extensive experimental investigations. The results obtained for four states of magnetofluidization and their applicability for collection of dust can be generalized briefly in the following manner.

1. The regime of a fixed bed lies within $U < U_{\min,f}$ and its characteristics depend on the quantity H. For example, the quantity ΔP increases with U for all values of H. At the same time, the quantities U and ΔP are independent of H in the region of weak magnetic fields, ΔP depends on H only slightly in the region of moderate magnetic-field intensities, and ΔP depends on H to a larger extent in the region of strong magnetic fields. Not only have these dependences of ΔP on U and H been revealed in our experiments, but they also agree with the data of [16] for the quantities H having values up to 40,000 A/m.

2. The regime of a partially stabilized bed is determined by the values of U lying in the range between $U_{\min,f}$ and $U_{\min,b}$, which is somewhat narrower in a weak magnetic field than in the magnetic field of moderate intensity. This is, possibly, due to the dependence of $U_{\min,b}$ on H. In such a regime, the particles of the bed are oriented along the magnetic lines and, if the external magnetic field is homogeneous, the bed acquires a stabilized and polymerized structure and the forces of interaction between the particles become larger than the forces of drag of the particles, with the result that a stabilized bed structure is maintained in the entire regime. According to our data and the data of [17], the quantity $\Delta P = W/A$ remains constant, no bubbles are formed, there is no particle motion, and expansion of the bed and increase in its porosity occur, the latter being higher in this regime than in the regime of a fixed bed.

3. The regime of a stabilized bed occurs when the velocity U is close to $U_{\min,b}$ and the magnetic-field intensity has a moderate value. The drag of the particles becomes comparable to the forces of interaction of the particles as a result of the high values of the gas velocity. In this regime, microinhomogeneities contributing to the agglomeration of the particles and formation of clusters or floccules of them are formed in the bed even with a homogeneous magnetic field. Such behavior becomes more pronounced with growth in H. As a result of the agglomeration of particles, their motion inside the bed is, to a certain extent, suppressed.

4. The regime of a frozen bed is observed for $0 > U_{\min,f}$, high intensities of the magnetic field, and large forces of interaction between particles. Large attracting forces lead to the coalescence of particles and the formation of a solid piston of them, which levitates at certain values of U. Before the bed begins to levitate, channels are formed in it, the quantity ε loses its conventional meaning, and the value of ΔP increases because of the increase in the velocity of the gas between the particles due to the reduction in the bed's height for the same velocity U, causing a decrease in the cross-sectional area for the gas motion.

Each of the magnetofluidization regimes observed, except for the regime of a fluidized bed with bubble nucleation, owing to the selection of the corresponding quantities U and H controlling the porosity of the bed, can, in principle, successfully be used for dust collection; as is clear from Fig. 4c, in the regime of a frozen bed, when the bed can be raised through a height h_2 above the gas distributor, the granular filter acquires an additional controlled volume for accumulation of dust, exceeding in certain cases the accumulating volume V_c of the bed itself.

On the basis of these investigations, we developed a scheme of delinearization (or a phase diagram) of states of the magnetofluidized bed (Fig. 5). If we plot the curves $U_{\min,f} = f(H)$ (1) and $U_{\min,b} = f(H)$ (2) representing visually fixed rates of transition of the magnetofluidized bed from a fixed state to a state of minimum fluidization and bubble nucleation and the curve $U_{\text{lev}} = f(H)$ (3), i.e., a visually observed velocity at which the bed rises above the gas-distributing grid in the form of a solid piston, we can classify the regions of magnetofluidized states as follows. Below the $U_{\min,f} = f(H)$ curve, there is the region of fixed-bed regimes. The region of fluidized-bed regimes with bubble nucleation is to the left of the $U_{\min,b} = f(H)$ curve, the region of frozen-bed regimes lies to the right of the $U_{\text{lev}} = f(H)$ curve, and, finally, the space between these curves determines the region of stabilized and partially stabilized regimes of magnetofluidization.

It emerged that the resistance of the bed for the quantities U lower than $U_{\min,f}$ depends on H only slightly and, for the regime of a fixed bed, can be based on evaluation of ΔP by the Carman–Kozeny formulation. The correlation in the form enjoying the widest use for calculation of ΔP can be written as

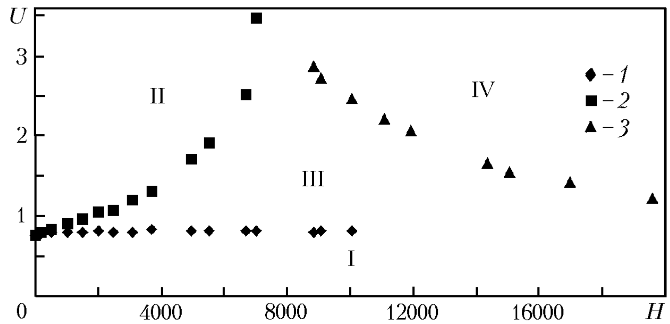

Fig. 5. Diagram of the regions of magnetofluidized-bed regimes: I) fixed bed; II) fluidized bed with bubbles; III) partially or completely stabilized magnetofluidized bed; IV) frozen bed. U, m/sec; H, A/m.

$$\Delta P = 150 \cdot \frac{(1-\varepsilon)^2}{\varepsilon^3} \frac{\mu_f U h}{d_s^2} + 1.75 \cdot \frac{1-\varepsilon}{\varepsilon^3} \frac{\rho_f U^2 h}{d_s} . \quad (12)$$

For the quantities $U > U_{\min,f}$ the value of ΔP is equal to W/A. Accurate determination of ΔP from Eq. (12) mainly depends on the accuracy with which ε has been determined. In actual fact, if ε is known for a particular value of H, Eq. (12) will yield quite an exact value of ΔP. The quantity ε was calculated from the experimental curves of resistance of the bed with increase and decrease in U. It has been revealed that the value of ε was higher in the case of reduction in the velocity U than in the case of its increase. Furthermore, experimental values of ε throughout the range of variation of the velocities and for the H values corresponding to the regimes of fixed, stabilized, and partially stabilized beds have a maximum spread of 11% of the average value, i.e., the same order of magnitude as the spread in ΔP values. On the basis of an analysis of the experimental values of ε and their dependence on H and U for the values equal to or higher than $U_{\min,f}$, for calculation of ε we proposed the following expression in general form:

$$\varepsilon = \varepsilon_o + 0.635 \mathrm{Ar}^{-0.334} (\mathrm{Re} - \mathrm{Re}_{\min,f})^{0.667} (1 - \varepsilon_o) \exp(-0.052 K_M) , \quad (13)$$

where

$$K_M = 1.5 \cdot \frac{\mu_0 H^2}{2 g \rho_s d_s} \quad (14)$$

is the characteristic parameter characterizing the influence of the magnetic field on the particle bed. The correlation proposed satisfies all the boundary cases of variation of U and H. A comparison of the experimental values of ε for the beds of irons spheres with an average diameter of 733 and 1511 μm and the values calculated from expression (13) shows that they are in good agreement.

Experimental values of the minimum rate of bubble nucleation $U_{\min,b}$ in the magnetofluidized bed have been determined from the data on the resistance of the bed with increase in the velocity U as a point of intersection of the $\Delta P = f(U)$ curve and W/A and the results obtained cannot be presented in the form of a linear plot. It is noteworthy that those values were somewhat lower than the actual rate of transition of a fixed bed to the onset of a fluidized state observed visually. Derivation of the correlation for calculation of $U_{\min,b}$ or $\mathrm{Re}_{\min,b}$ is a complex process, since it must include knowledge of the properties of solid particles and a fluidizing medium and of the parameters characterizing the influence of the magnetic field applied on the bed of solid particles. As a result of an analysis of the experimental data obtained on the quantities $U_{\min,b}$ and their dependence on H up to values of 10,000 A/m, we proposed the correlation

$$\mathrm{Re}_{\min,b} = \mathrm{Re}_{\min,f} + 2.25 \cdot 10^{-3} K_M^{0.59} \mathrm{Ar}^{0.81} \quad (15)$$

TABLE 3. Range of the Coefficients of Protective Action of a Magnetofluidized Bed $k_p = \tau_{max}/\tau_{min}$ of Iron Spheres (d_s = 0.733 mm) in Collection of Talc (d_d = 2 μm)

H, A/m	$U - U_t$, m/sec	C, g/m^3						
		1.79	2.06	2.4	2.87	3.58	4.76	7.15
		Partially stabilized magnetofluidized bed						
12,730	1.240	4.01339	3.48737	2.99332	2.50313	2.00670	1.50924	1.00475
	1.277	3.99441	3.47087	2.97917	2.49129	1.99721	1.50210	1.00000
2785	1.240	4.35117	3.78087	3.24525	2.71379	2.17558	1.63626	1.08931
	1.304	4.15647	3.61169	3.10004	2.59236	2.07824	1.56304	1.04057
	1.367	3.99441	3.47087	2.97917	2.49129	1.99721	1.50210	1.00000
3740	1.256	4.77073	4.14544	3.5582	2.97547	2.38537	1.79404	1.19435
	1.307	4.60481	4.00126	3.43442	2.87199	2.30240	1.73164	1.15281
	1.436	4.27224	3.71229	3.18638	2.66457	2.13612	1.60657	1.06955
	1.565	3.99441	3.47087	2.97917	2.49129	1.99721	1.50210	1.00000
5013	1.272	5.00875	4.35226	3.73569	3.12392	2.50437	1.88354	1.25394
	1.327	4.83662	4.20270	3.60731	3.01657	2.41831	1.81881	1.21085
	1.443	4.50092	3.91100	3.35693	2.80719	2.25046	1.69257	1.12680
	1.568	4.22815	3.67398	3.15350	2.63707	2.11408	1.58999	1.05852
	1.690	3.99441	3.47087	2.97917	2.49129	1.99722	1.50210	1.00000
7162	1.288	5.55567	4.82744	4.14355	3.46499	2.77780	2.08919	1.39084
	1.423	5.11089	4.44102	3.81187	3.18763	2.55545	1.92195	1.27951
	1.555	4.74231	4.12075	3.53697	2.95775	2.37115	1.78335	1.18724
	1.690	4.49301	3.90412	3.35104	2.80226	2.24651	1.68959	1.12482
	1.819	4.20282	3.65196	3.13460	2.62127	2.10141	1.58047	1.05217
	1.948	3.99441	3.47087	2.97917	2.49129	1.99721	1.50210	1.00000
		Completely stabilized magnetofluidized bed						
9072	1.288	6.68872	5.81205	4.98867	4.17171	3.34436	2.51530	1.67452
	1.317	6.69367	5.81634	4.99236	4.17480	3.34683	2.51716	1.67576
	1.443	6.24985	5.43069	4.66134	3.89799	3.12492	2.35026	1.56465
	1.573	5.85906	5.09113	4.36988	3.65426	2.9295	2.20330	1.46681
	1.690	5.57023	4.84015	4.15447	3.47412	2.78512	2.09469	1.39451
	1.819	5.28600	4.59318	3.94248	3.29685	2.64300	1.98780	1.32335
	1.948	5.03936	4.37886	3.75852	3.14302	2.51968	1.89505	1.26160
	2.077	4.82331	4.19113	3.59738	3.00827	2.41165	1.81381	1.20751
	2.206	4.63249	4.02532	3.45506	2.88925	2.31624	1.74205	1.15974
	2.608	3.99441	3.47087	2.97917	2.49129	1.99721	1.50210	1.00000
10,026	1.320	6.76637	5.87951	5.04658	4.22014	3.38318	2.54449	1.69396
	1.359	6.78240	5.89344	5.05854	4.23014	3.39112	2.55052	1.69797
	1.513	6.27688	5.45419	4.68151	3.91485	3.13844	2.36043	1.57142
	1.660	5.89350	5.12105	4.39557	3.67574	2.94675	2.21625	1.47544
	1.727	5.82677	5.06307	4.34580	3.63412	2.91338	2.19116	1.45873
	1.900	5.44750	4.73351	4.06293	3.39757	2.72375	2.04853	1.36378
	2.124	5.00680	4.35057	3.73424	3.12271	2.50340	1.88281	1.25345
	2.333	4.67902	4.06575	3.48977	2.91827	2.33951	1.75955	1.17139
	2.798	3.99441	3.47087	2.97917	2.49129	1.99721	1.50210	1.00000

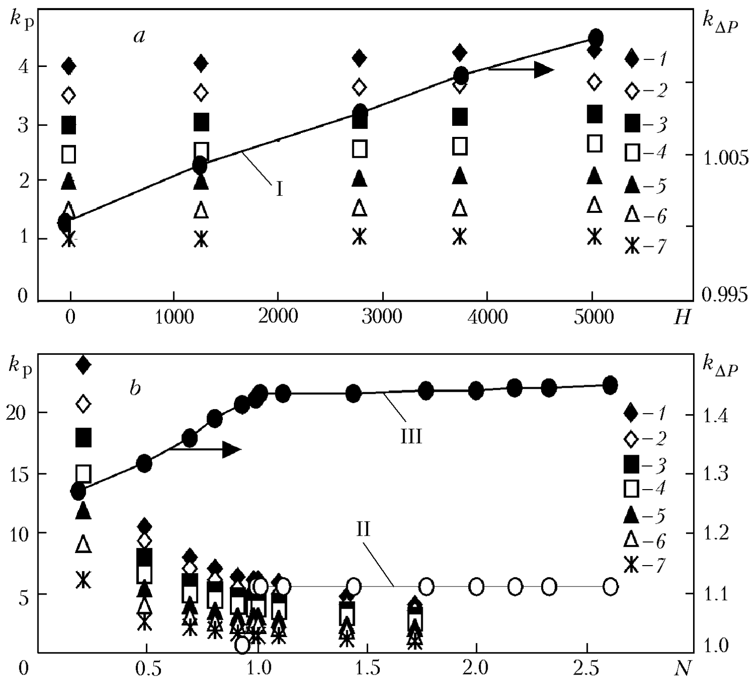

Fig. 6. Collection of dust in the regime of a fixed bed (a) and a magnetofluidized bed (b) at N = 0.818 (a), H = 5013 A/m (b), and T_c = 200°C: 1) C = 1.79; 2) 2.06; 3) 2.4; 4) 2.87; 5) 3.58; 6) 4.76; 7) 7.15 g/m^3 [I) $k_{\Delta P} = f(H)$; II) $k_{\Delta P} = f(N)$ under experimental conditions; III) $k_{\Delta P} = f(N)$ for H = 0 and C = 0]. d_s = 1.511 mm, iron spheres, d_d = 20 μm, corundum. H, A/m.

for calculation of $U_{\min,b}$.

A comparison of our experimental data on $\mathrm{Re}_{\min,b}$ and of those obtained in [3, 18] to the corresponding quantities calculated from expression (15) demonstrates their good agreement with a spread of ±10%.

Determination of the quantity $U_{\min,f}$ is not complicated by the external magnetic field and consequently it can be calculated from the well-known correlation [1]

$$\mathrm{Re}_{\min,f} = \frac{\mathrm{Ar}}{1400 + 5.22\sqrt{\mathrm{Ar}}} \tag{16}$$

or be determined from the experimental data on the dependence of ΔP on U.

Efficiency of Removal of Dust from Hot Gases by a Magnetofluidized Filter. According to the procedure described above, we carried out extensive investigations on collection of dust by the bed in all four regimes of magnetofluidization revealed. In this section, we discuss the results obtained.

The prime objective of these systematic investigations is experimental study of the influence of a number of such variable parameters as the intensity of a magnetic field, the gas velocity, the bed's height, the concentration of dust in the inlet flow, the temperature of the air flow, and the size of particles in the bed and of those of the collected dust on the operating characteristics of dust collection and the resistance of a magnetofluidized bed.

Experimental data were processed in the form of the functions $k_p = f(N)$ and $k_{\Delta P} = f(N)$, i.e., in the form of the so-called coefficients of protective action of the bed $k_p = \tau_{\max}/\tau_{\min}$ and the coefficients of resistance of the bed $k_{\Delta P} = \Delta P_{\max}/\Delta P_{\min}$ for this range of variation of the quantities U, H, C, d_s, and d_d. The period of time up to the instant of the appearance of re-removal due to the suffosion from the upper interlayers of the bed (in the vicinity of the state of complete clogging of the bed) and for $N = (U - U_t)/U_{\min,f}$ was taken as the time of protective action of the bed. The appearance of re-removal of dust was recorded by scanning of the space above the bed by a laser beam. The final results are presented in Table 3 and Figs. 6–8.

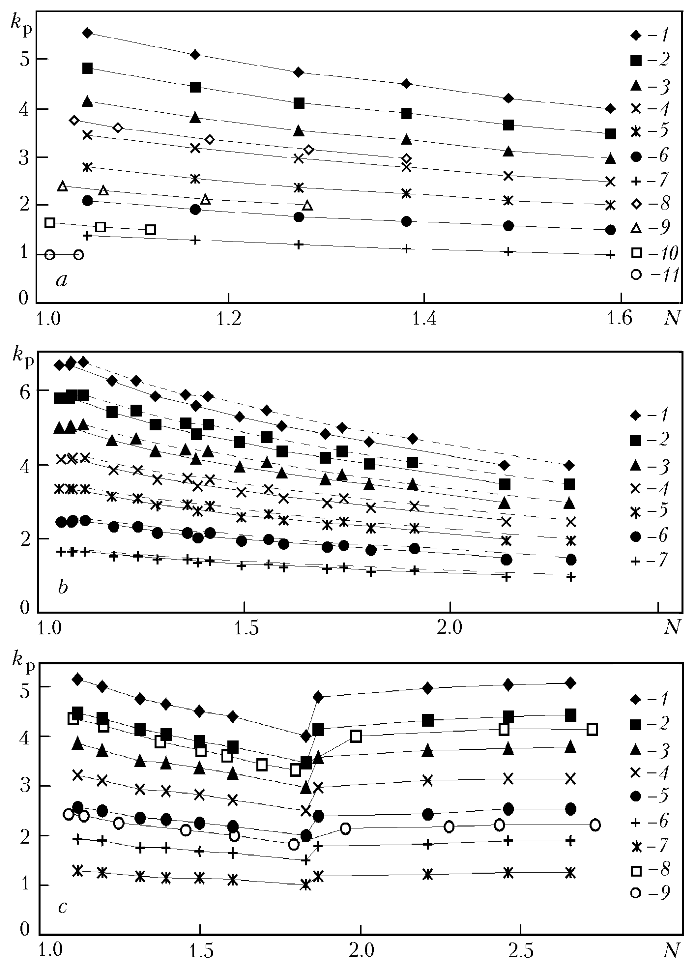

Fig. 7. Collection of dust in the regimes of partially stabilized (a), stabilized (b), and frozen (c) magnetofluidized beds in the range of velocities $U_{min,f} \le U - U_t \le U_{min,b}$: 1) C = 1.79; 2) 2.06; 3) 2.4; 4) 2.87; 5) 3.58; 6, 10) 4.76; 7, 11) 7.15; 8) 2.4 (a) and 2.06 (c); 9) 3.58 g/m^3 [a: 1–7) H = 7162; 8) 5013; 9) 3740; 10) 2875; 11) 1273 A/m; b) solid curve, H = 9072 A/m; dashed curve, H = 10,026 A/M; c: 1–7) H = 19,576; 8) 16,950; 9) 14,324 A/m). d_s = 0.733 mm, iron spheres, d_d = 2 μm, talc, and T = 200^{o}C.

Magnetofluidized filters can, in principle, operate in the regime of a fixed bed (Fig. 6a) throughout the intensity range of the magnetic fields applied. In the range of a weak magnetic field, this regime is limited to the interval of gas velocities $U < U_{min,f}$. But the region of operating velocities extends with growth in the magnetic-field intensity, and in the region of strong magnetic fields (14,000 $\le H \le$ 20,000 A/m), the bed is in a fixed state throughout the range of the investigated velocities, in practice. In this regime, as the velocity range grows, the time of protective action of the bed and its resistance in the region of weak, moderate, and strong magnetic fields lead to a growth of 12% in Δ_U, 15% in Δ_τ, and 12.5% in $\Delta_{\Delta P}$. However, if the bed is assumed to be in a fixed state in the region of strong magnetic fields, these quantities will be even larger.

Operation of a magnetofluidized filter in the regime of a partially stabilized bed (Fig. 7a) is characterized by a range of velocities somewhat higher than $U_{min,f}$ and weak and moderate intensities of the magnetic field. Growth in the value of H in this regime leads to a certain extension of the range of operating velocities and flow rates of the gas, and the increase in the ranges of gas velocities, protective action of the bed, and resistance attains 59, 20, and 4% respectively.

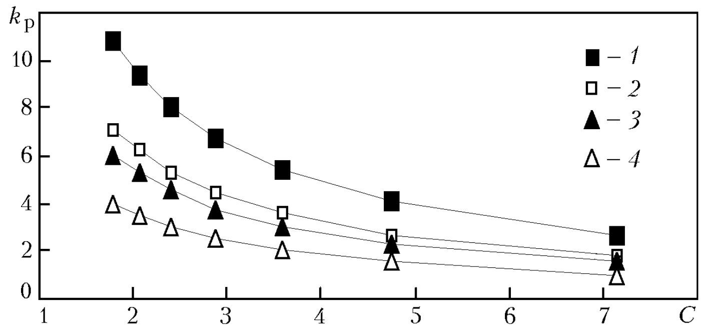

Fig. 8. Comparison of the data on collection of dust in a magnetofluidized bed for particles of different size: 1) d_s = 0.733 and d_d = 2; 2) 0.733 and 20; 3) 1.511 and 2; 4) 1.511 mm and 20 μm. H = 5013 A/m, N = 1.53, and T_c = 250°C. C, kg/m^3.

Operation of a magnetofluidized filter in the regime of a stabilized bed (Fig. 7b) extends to the range of velocities lying between $U_{min,f}$ and $U_{min,b}$ and to moderate intensities of the magnetic field. Increase in H in this regime leads to a certain suppression of the nucleation of bubbles inside the bed and a growth in operating velocities up to the occurrence of re-removal of dust. In this regime, the increase in the ranges of flow rates of the gas, protective action of the bed, and resistance attains 140, 33, and 6% respectively.

Operation of a magnetofluidized filter in the regime of a frozen bed (Fig. 7c) occurs for $U > U_{min,f}$ and very strong magnetic fields. Growth in the gas velocity above $U_{min,b}$ in this regime leads to a rise of the bed above the gas distributor and the formation of an additional useful accumulating volume in the filter. In this regime, the increase in the ranges of flow rates of the gas, protective action of the bed, and resistance attains 175, 140, and 25% respectively.

The results obtained quite clearly demonstrate the influence of variable operating parameters on the basic characteristics of a magnetofluidized filter, in particular, on the time of protective action of the bed τ_p and its resistance ΔP. As is clear from the data presented, growth in the concentration of dust C in a hot air flow for the same U, H, d_s, and d_d leads to a reduction in τ_p due to the increase in the amount of dust fed by the flow to the bed per unit time. An increase of U at the same C, H, and other variables leads to a decrease of τ_p. Growth in H leads to a growth in the value of τ_p due to the restructuring of the bed under the action of magnetic forces and a growth in ε in the accumulating volume inside the bed V_c. At the same time, a twofold increase in the size of the bed particles d_s and a tenfold increase in the size of the dust particles d_d leads to a nonmonotonic reduction in τ_p due to the certain decrease in the porosity of the bed ε and the increase in the volume of a single dust particle, according to experimental data (Fig. 8).

As far as the resistance of the filter is concerned, the ΔP curves in magnetofluidization follow, as a rule, typical "curves of fluidization" in the bed for H = 0 but lie somewhat above because of the additional mass of the dust collected by the bed (see Fig. 6b). The influence of the basic operating variables on the resistance of the filter preserves, in principle, the same tendencies as in the previous cases, with the exception of the influence of the gas velocity, when this tendency becomes opposite. Increase in the density of the gas ρ_d leads to a growth in ΔP.

Thus, the investigations performed demonstrate that application of an external magnetic field to a bed of magnetosensitive particles is very attractive for using such beds as granular filters owing to their advantages in increasing the ranges of operating flow rates of the gas and the time of protective action of the bed.

Physicomathematical Modeling and Calculations. The theoretical and experimental investigations performed have enabled us to create physicomathematical models of the processes of decontamination of volatile organic substances and collection of dust from industrial waste gases and to develop computer programs for their calculation that made it possible to simulate these processes under nearly actual conditions and to optimize the operating and structural parameters of gas-purification systems. Description of these models and programs is beyond the scope of this work.

Use of the Results Obtained. The wide range of theoretical and experimental investigations given above became a basis for the development of a modern energy-resource-saving gas purification technology (which urgent is for

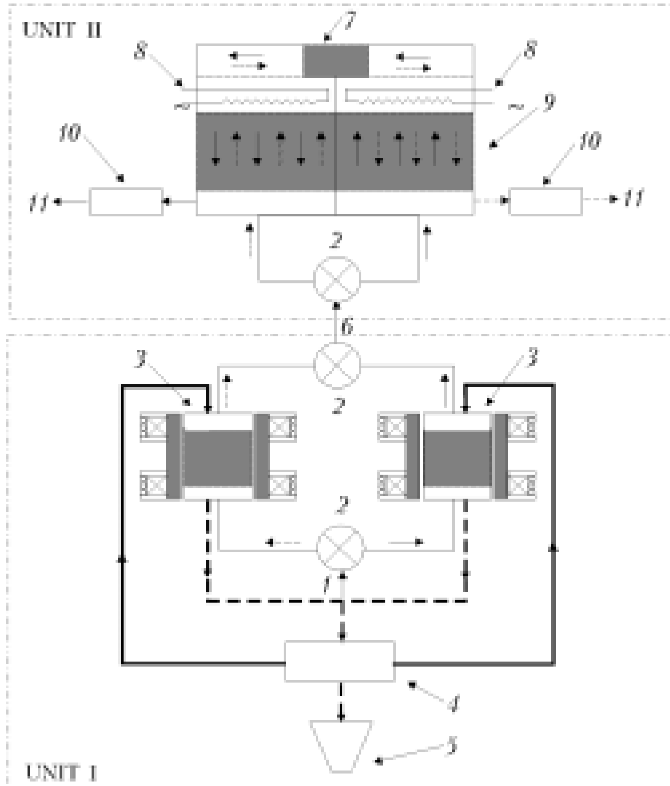

Fig. 9. Gas-purification device for simultaneous removal of volatile organic substances and dust from hot gases: I) unit of cleaning of hot waste gases of dust particles [1) hot waste gas contaminated by dust and volatile organic substances; 2) selector valves; 3) filters with a magnetofluidized bed; 4) regenerator of filter particles; 5) dust collector]; II) unit of catalytic cleaning of volatile organic substances [6) waste gas contaminated by organic substances; 7) catalyst unit; 8) heaters; 9) accumulator of heat; 10) recuperators of heat; 11) cleaned gas to be exhausted].

many industries) for simultaneous removal of dust and volatile organic substances from high-temperature waste gas flows.

According to Fig. 9, the gas-purification equipment proposed consists of two units combined in one device: a unit of catalytic decontamination of organic pollutants and a unit of a magnetofluidized granular filter for cleaning of gases of dust.

The waste gas to be cleaned of gaseous and solid substances first arrives at a filter with a magnetofluidized bed where it is cleaned of dust. Depending on the flow rate of the gas, the concentration of dust, and the operating time of the basic equipment, the unit can contain one or two filters with a magnetofluidized bed. In the cases where the operating time of the basic equipment corresponds to the estimated time of protective action of the bed, use is made of one magnetofluidized filter. If the operating time of the basic equipment and the concentration of dust in the flow are too high, two filters must be used in this unit. In the case where one filter is completely clogged with dust, a valve sensitive to pressure growth automatically switches the gas-feeding line to the second filter, whereas the first filter passes to the stage of regeneration of the bed particles. Separation of the bed and dust particles and accordingly regeneration of a filter medium can be carried out in any separator intended for these purposes. Any magnetosensitive particles whose Curie point is higher than the temperature of hot waste gases can be used as the bed particles. Thus, the process of purification of the hot waste gas is carried out in each of the two magnetofluidized filters in turn.

After the removal of dust, the waste gases containing organic substances arrive at the catalyst unit for deep thermocatalytic oxidation of organopollutants. If the temperature of the hot waste gas is sufficient for catalytic oxidation of the organic matter by the catalysts used, there is no need for heat accumulators in this unit and the internal heat of the gas itself is used as the heat for the process of oxidation. If the temperature of the waste gases is insufficient for the oxidation, the catalyst unit is equipped with two heaters and heat accumulators of granular or another type. In this case, the shortage of heat required for complete oxidation of the organic matter in the catalyst unit is made up for by the heaters and is saved in the heat accumulators to reduce the heat loss and operating costs. The two accumulators of heat operate in the regime of accumulation and sink of heat in turn: when the first accumulator is cooled down to a prescribed temperature, it is put out of operation and the second accumulator begins to operate as an additional heat source. Any catalysts whose temperature range of oxidation of the organic matter is the closest to the temperature of the hot waste gases can be used in this unit as catalytic materials.

CONCLUSIONS

On the basis of a wide range of theoretical and experimental investigations, we:

(1) have shown that the application of an external magnetic field on a bed of magnetosusceptible particles makes it possible to control and substantially increase the accumulation volume and the time of protective action of a magnetofluidized filter as compared to the existing granular filters;

(2) have constructed a phase diagram of magnetofluidization states;

(3) have proposed correlations for calculation of certain basic parameters of magnetofluidized filters with an accuracy of $\pm 10\%$ that generalize the data of other authors;

(4) have developed physicomathematical models and computer programs of calculation of gas-purification processes that make it possible to optimize the operating and structural parameters of gas-purification systems;

(5) have proposed a new energy-resource-saving technology of gas purification for simultaneous removal of solid and gaseous substances from high-temperature waste gases and have proved the high prospects for its use in many industries contaminating the environment with toxic organic substances and dust.

NOTATION

A, cross-sectional area of the bed, m^2; A_s, dimensionless parameter dependent on the porosity of the bed and determined as $2(1-P^5)/P'$, where $P = (1-\varepsilon)^{1/3}$ and $P' = 2 - 3P + 5P^5 - 2P^6$; $\mathrm{Ar} = [gd_s^3(\rho_s - \rho_f)]/\rho_f\nu^2$, dimensionless Archimedes number; C, running concentration of dust, kg/m^3; C_{in} and C_{of}, inlet and outlet concentrations of dust particles, kg/m^3; d_c^*, dimensionless diameter of the pores; d_d, diameter of the dust particles, mm; d_s, diameter of the bed particles, mm; D, coefficient of Brownian diffusion, m^2/sec; E, dimensionless total efficiency of dust collection of the filter; g, free fall acceleration, m/sec^2; h, height of the particle bed in the filter, m; h_1, height of the subgrid space for accumulation of dust, m; h_2, height of rise of the bed above the grid under the action of aerodynamic and magnetic forces, m; H, strength of the external magnetic field, A/m; k_p, dimensionless coefficient of protective action of the bed; $k_{\Delta P}$, dimensionless coefficient of resistance of the bed; K_M, characteristic parameter; l_c, axial distance to a single collector in the bed, m; M_0, magnetization of the particles in a fluidized state, A/m; m_c, mass of the dust particles collected in the filter, kg; $N = U/U_{min,f}$, dimensionless fluidization number; $N_G = [d_d^3(\rho_d - \rho_f)gCA]/[18\mu_f d_s]$, dimensionless gravitation parameter; $N_{Pe} = d_s w/D$, dimensionless Péclet number; $N_R = d_d/d_s$, dimensionless parameter determined by the relative size of the dust and bed particles; N_{Re_s}; dimensionless Reynolds number for particles in Eq. (11); $N_{St} = d_d^2 U\rho_d CA/\mu_f d_s$, dimensionless Stokes number; $\mathrm{Re} = d_s U\rho_f/\mu_f$, dimensionless Reynolds number; $\mathrm{Re}_{min,f} = d_s U_{min,f}\rho_f/\mu_f$, dimensionless Reynolds number of minimum fluidization; T, temperature of the bed in catalytic oxidation of the organic matter, ^{o}C; T_c, collection temperature, ^{o}C; U, gas velocity, m/sec; $U_{min,b}$, minimum rate of bubble nucleation, m/sec; $U_{min,f}$, rate of minimum fluidization of particles, m/sec; U_t, free-fall velocity of particles, m/sec; V_{bed}, total volume of the bed, m^3; V_c, accumulating volume of the bed for collection of dust, m^3; V_1, accumulating volume below the gas-distributing grid, m^3; V_s, volume of the bed particles, m^3; w, intensity of circulation of particles in the bed, kg/sec; W, mass of the bed particles, kg; $x_0 = dM_0/dH$, dimensionless magnetic susceptibility of particles; $\Delta_{\Delta P}$, increment in the resistance of the filter, MPa; Δ_τ, increment in the time of protective action of the filter, sec; Δ_U, increment in the range of operating velocities (flow rates) of the gas in the filter, m/sec; ΔP, hydrodynamic resistance of the bed, MPa; ΔP_{max} and ΔP_{min}, maximum and minimum resistances of the bed, MPa; ε, dimensionless running porosity of the bed; ε_o, dimensionless porosity of a fixed bed; ε_d, dimensionless porosity of the collected dust; η, efficiency of collection of dust by the filter, %; $(\eta_0)_G$, efficiency of collection of dust under gravity; $(\eta_0)_D$, efficiency of collection of dust under the action of Brownian diffusion; $(\eta_0)_I$, efficiency of collection of dust under the action of the collisions of the filter and dust particles; $(\eta_0)_{i,I}$, efficiency of collection of dust under the action of the collisions of particles and trapping of dust; λ, collection coefficient of the filter; $\mu_0 = 4\pi\cdot10^{-7}$, permeability of the medium in vacuum, N/m; μ_f, dynamic viscosity of the fluidizing medium, N·sec/m^2; ν, kinematic viscosity of the fluidizing medium, m^2/sec; ρ_f, density of the fluidizing medium, kg/m^3; ρ_d, density of the dust particles, kg/m^3; ρ_s, density of the bed particles, kg/m^3; τ_{max} and τ_{min}, maximum and minimum times of protective action of the bed, sec; τ_p, time of protective action of the bed, sec. Subscripts: b, bubble, bubble nucleation; bed, bed; c, collection; d, dust particles; f, fluidizing medium; in, inlet parameter; lev, levitation (rise of the bed); max; maximum value; min, minimum value; o, fixed bed; of, outlet parameter; p, protective action; s, bed particles; t, free fall (flotation).

REFERENCES

1. M. É. Áerov and O. M. Todes, *Hydraulic and Thermal Principles of Operation of Apparatuses with Stationary and Fluidized Granular Beds* [in Russian], Khimiya, Leningrad (1968).
2. P. Knettig and J. M. Beeckmans, Capture of monodispersed aerosol particles in a fixed and in a fluidized bed, *Can. J. Chem. Eng.*, **52**, 703–706 (1974).
3. J. J. Neff and B. Rubinski, The effect of a magnetic field on the heat transfer characteristics of an air fluidized bed of ferromagnetic particles, *Int. J. Heat Mass Transfer*, **26**, No. 12, 1885–1889 (1983).
4. A. F. Dolidovich, V. L. Ganzha, S. C. Saxena, and S. H. Rahman, The magnetic field effect on the particle behavior and heat transfer between an immersed horizontal tube and a gas magnetofluidized bed, in: *Proc. Eur. Conf. "Fluidization-3,"* May 29–31, 2000, Toulouse, France (2000), pp. 1002–1111.
5. H. Katz and J. T. Sears, Electric field phenomena in fluidized and fixed beds, *Can. J. Chem. Eng.*, **47**, 50–56 (1969).
6. R. E. Rosensweig, Process for Operating a Magnetically Stabilized Fluidized Bed, U.S. Patent No. 4,1 15, 927 (1978).
7. R. E. Rosensweig, Fluidization hydrodynamic stabilization with a magnetic field, *Science*, **204**, 57–61 (1979).
8. S. C. Saxena, V. L. Ganzha, S. H. Rahman, and A. F. Dolidovich, Heat transfer and relevant characteristics of magnetofluidized beds, *Adv. Heat Transfer*, **25**, 151–249 (1994).
9. R. L. Sonolikar, S. G. Ingle, J. R. Giradkar, and P. S. Mene, Influence of magnetic field on fluidization of iron particles, *Indian J. Tech.*, No. 10, 377–384 (1972).
10. Yu. I. Tambovtsev and S. S. Zabrodskii, Study of the structure of a ferromagnetic fluidized bed by measuring its magnetic characteristics, *Inzh.-Fiz. Zh.*, **32**, No. 1, 34–44 (1977).
11. S. S. Zabrodskii and Yu. I. Tambovtsev, *Method of Creation of a Fluidized Bed from Ferromagnetic and Nonmagnetic Particles*, USSR Inventor's Certificate No. 842103, Moscow (1981).
12. R. V. Albert and C. Tien, Particle collection in magnetically stabilized fluidized filters, *AIChE J.*, **31**, No. 2, 288–295 (1995).
13. M. Warrior and C. Tien, Experimental investigation of aerosol filtration in magnetically stabilized fluidized bed filters, *Chem. Eng. Sci.*, **41**, No. 7, 1711–1721 (1986).
14. A. F. Dolidovich, G. S. Akhremkova, and V. S. Efremtsev, Novel technologies of VOC decontamination in fixed, moving and fluidized catalyst-adsorbent beds, *Can. J. Chem. Eng.*, **77**, 342–355 (1999).
15. R. Rajagopalan and C. Tien, Trajectory analysis of deep bed filtration using the sphere-in-cell porous media model, *AIChE J.*, **22**, 523–531 (1976).
16. I. A. Zrunchev and T. F. Popova, Magnetic technology of heterogeneous processes — Basic principles, *Izv. Khim.*, **21**, No. 4, 484–490, Sofia (1988).
17. P. U. Foscolo and L. G. Gibilaro, A fully predictive criterion for the transition between particulate and aggregative fluidization, *Chem. Eng. Sci.*, **39**, No. 12, 1667–1675 (1984).
18. M. K. Bologa and S. V. Syutkin, The influence of an electromagnetic field on the structural-hydrodynamic properties of a fluidized bed, *Elektron. Obrab. Mater.*, No. 1, 37–42 (1977).